Cluster stability driven by quantum fluctuations

Cluster stability driven by quantum fluctuations

Fabio Cinti *

Department of Physics and Astronomy, University of Florence, Via Sansone 1, I-50019, Sesto Fiorentino (FI), Italy and Department of Physics, University of Johannesburg, P.O. Box 524, Auckland Park 2006, South Africa

(Received 7 August 2019; revised manuscript received 22 November 2019; published 27 December 2019)

By means of an accurate path-integral Monte Carlo, we investigate a two-dimensional ensemble of particles interacting via a Lifshitz-Petrich-Gaussian potential. In particular, analyzing structures described by a commensurate ratio between the two wave numbers that mark the pattern, the Lifshitz-Petrich-Gaussian boson model may display a stable and well-defined stripe phase lacking any global phase coherence but featuring a superfluid signal along the stripe direction only. Upon increasing quantum fluctuations and quantum-mechanical exchange of bosons, the double-degeneration of the negative minima in the Fourier transform of the potential is removed at the expense of a density modulation peculiar to a cluster triangular crystal. We also show that this last structure possess all features adhering to the definition of a supersolid phase.

DOI: 10.1103/PhysRevB.100.214515

I. INTRODUCTION

The physical properties of cluster phases is progressively becoming a pivotal aspect in condensed and soft matter as well as in atomic physics. Particle aggregates show properties, whose features can be mainly described microscopically by means of effective potentials and, at equilibrium, they can self-organize in nontrivial structures [1,2]. This allows us to design and experimentally control such structures at different length and energy scales. In a pure classical context, it is already well established that the necessary mathematical condition to aggregate particles into cluster phases is that the Fourier transform of the effective two-body potential must exhibit at least a negative minimum [3,4].

In the context of soft matter and biological systems, much work as been already done by successfully using generalized exponential models which are capable of accounting the behavior of colloids and polymer chains [5–7]. Such models can introduce patterns by balancing between repulsive forces at short range (particles in a cluster) and those at long range (or intermediate long range), affecting the rest of the structure. More interestingly, the pattern symmetry would generate spherical, cylindrical, sheetlike, inverted, or even bicontinuous structures [4,8–11]. Moreover, in some cases, the interplay between different lengthscales may also produce quasicrystal phases [12].

Very recently, Barkan *et al.* [13] has designed a set of isotropic pair potentials which are capable of assembling rich wealth of ordered equilibrium structures such as, for instance, stripes or quasicrystals. Interestingly, such two-body potentials furnish a Fourier transform exhibiting an instability at two different wave numbers. If the ratio between the wave numbers is an integer (or more generically a rational number), the potential describes a stripe phase [14,15]. Otherwise, if the ratio turns out to be irrational, one obtains quasicrystals with a ten- and 12-fold symmetry.

Considering particles obeying quantum statistics, the corresponding many-body physics of quantum aggregates is indeed paving the way to new and challenging phases of matters. By way of illustration, alkaline atoms off-resonantly excited to Rydberg states furnish two-body soft-shoulderlike shape potentials that may show quantum clusters which result to be identified as an example of supersolid phase [16–20]. Furthermore, it has been pointed out that a Bose system interacting via a pairwise potential composed of a repulsive core at short distances furnishes quantum-mechanical exchanges that stabilize triangular cluster phases at finite temperature in a wider region of parameter space than predicted by calculations in which exchanges are neglected [21]. Regarding systems made up of fermions, it has been shown in Ref. [22] there exits a competition between quantum-liquid and electron-solid (cluster) phases for some Landau levels by varying the filling factor.

Quantum aspects of quasicrystals with a dodecagonal symmetry have been discussed in Ref. [23]. In particular, the authors observed that a quantum quasicrystal still maintains the dodecagonal pattern as well as a small yet finite superfluidity signal. Moreover, large quantum fluctuations induce a transition to a triangular cluster and then to a supersolid phase. Such a dynamic may lead to other unforeseen behaviors if quantum effects are taken into account. It is worthwhile to mention that the debate concerning the intrinsic properties of quantum stripe patterns still remains open. As an example, Masella *et al.* [24] have recently faced the problem on a lattice. They found that the competition between quantum fluctuations and cluster formation may give an anisotropic stripe supersolid phase.

Here we propose an innovative theoretical investigation considering an ensemble of bosons interacting with a Lifshitz-Petrich-Gaussian (LPG) pair potential. The study pays special attention to commensurate patterns such as the above-mentioned stripe phase. We use path-integral Monte Carlo

*fabio.cinti@unifi.it

(PIMC) simulations to show that stripe phase remains stable if quantum fluctuations are not too large and without supporting any global superfluidity but showing a phase coherence along stripes only. Boosting fluctuations up, we observe, before a complete melting, an unexpected structural transition to a triangular cluster crystal. This last phase is indeed a supersolid.

The rest of the paper is organized as follows: In Sec. II, we introduce the Lifshitz-Petrich-Gaussian pair potential as well as the microscopic model describing the stripes phase in the quantum regime. Section II also outlines the numerical methodology employed as well as the estimators of the thermodynamic observables. In Sec. III, we illustrate our results, whereas conclusions will be reported in Sec. IV.

II. MODEL, METHODOLOGY AND THERMODYNAMIC OBSERVABLES

We consider the LPG pair potential [13], defined as

$$U(r) = e^{-\frac{1}{2}\sigma^2 r^2}(C_0 + C_2 r^2 + C_4 r^4 + C_6 r^6 + C_8 r^8). \quad (1)$$

In the present paper, we pick the parameters σ and C_i such that the a classical equilibrium configuration at low temperature forms a striped pattern. Figure 1(a) shows the pair potential. Fourier transform [Fig. 1(b)] of Eq. (1) furnishes two equal-depth negative minima with a corresponding ratio of commensurate wave-vectors $k = 2$ [13]. As previously mentioned, we aim to investigate how quantum effects may alter this particular pattern. For this purpose, we consider a two-dimensional system composed of N spin-zero bosons of mass m. So the Hamiltonian describing the quantum-mechanical system reads

$$H = -\frac{\hbar^2}{2m}\sum_{i=1}^{N}\nabla_i^2 + \sum_{i<j}^{N} U(\mathbf{r}_{ij}), \quad (2)$$

where the first term of Eq. (2) regards the kinetic contribution to the total energy whereas the second sum refers to the two-body potential Eq. (1), being $\mathbf{r}_{ij} = |\mathbf{r}_i - \mathbf{r}_j|$ and $\mathbf{r}_i \equiv (x_i, y_i)$ the position of ith bosons on the plane, respectively.

To properly quantify the influence of the quantum fluctuations, we introduce the so-called de Boer parameter [25],

$$\Lambda = \sqrt{\frac{\hbar^2}{m r_0^2 U_0}}, \quad (3)$$

where U_0 is the pair potential at $r = 0$ and r_0 is the characteristic length given by the inverse of the wave vector corresponding to the first minimum of the Fourier transform of $U(r)$. In a crystal, the de Boer term accounts for zero-point vibrations in the limit for $T \to 0$. Depending on the material under investigation, by increasing Λ the crystal becomes unstable with respect to zero-point motion even at $T = 0$, usually referred to as quantum melting. Λ is particularly useful to study quantum fluctuation on quantum fluids like He, Ne, and H_2 [26].

We investigated the equilibrium properties of the system described by the Hamiltonian Eq. (2), employing first-principles computer simulations based on a continuous-space PIMC [27,28]. The calculations include the use of the *worm algorithm* (WA), which allows one to obtain the exact

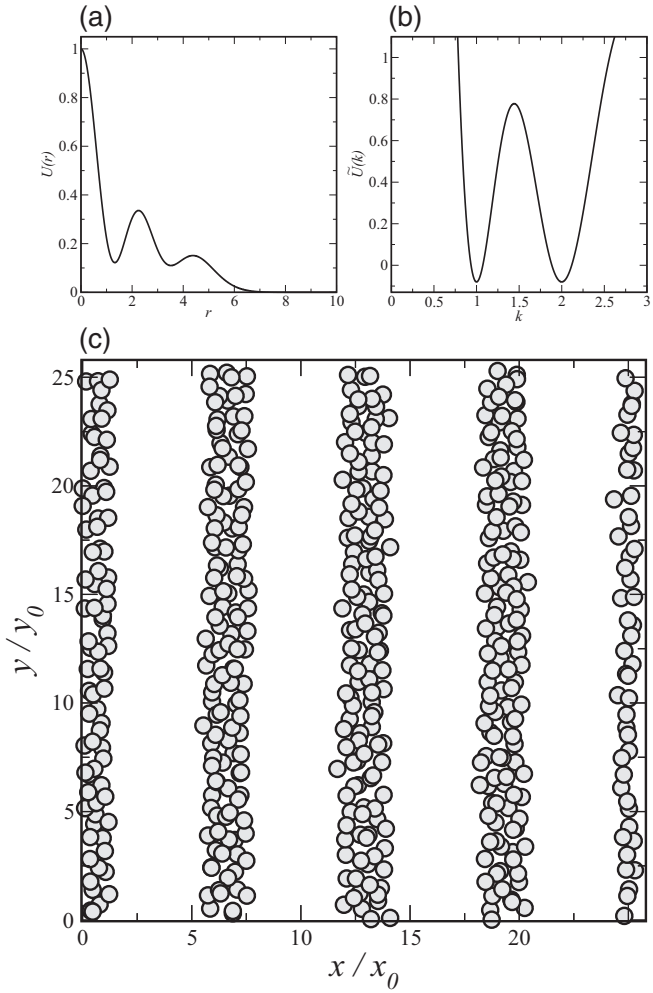

FIG. 1. (a) Lifshitz-Petrich-Gaussian pair potential of Eq. (1) in real space. Parameters σ and C_i have been taken from Ref. [13]. (b) Fourier transform of Eq. (1). The panel shows a close view of the minima characterizing the classical stripe pattern (c) Snapshot of a stripe phase composed by classical particles interacting via the two-body potential in (a). The result has been obtained employing a classical Monte Carlo using 512 particles at temperature $t = 0.03$.

thermodynamics properties of a bosonic system. WA has been successfully tested on a large variety of systems, including 4He [29], Rydberg atoms [17,30], and dipolar systems [31–33]. The reader may consult Ref. [34] for a thorough illustration of the methodology. Here we shall only give a few details concerning the approximation applied on the density operator. Given the fact that the LPG potential in Fig. 1(a) does not feature any dramatic discontinuity, being a smooth analytical function, it is perfectly appropriate to apply a fourth-order expansion of the density operators already proposed a while ago by Chin in Ref. [35]. The expansion takes into account the first derivatives of the interparticle potential and it has the great advantage of evaluating the density operators with a small number of time slices, even at low temperature.

We have worked to find out the equilibrium state of Eq. (2) at a fixed temperature and number of particles N (canonical ensemble), with N between 256 and 1024. Simulations are

performed using periodic boundary conditions along x and y directions. The de Boer parameter is considered in the range between 0 and 1, whereas we set the reduced temperature at $t = k_B T/U_0 = 0.03$.

Concerning the system's density, as one can suppose for the two-body potential here introduced, the kind of pattern that is accomplished at equilibrium is going to result strongly affected by this parameter. Consistently with molecular dynamic simulations discussed in Ref. [13], it is expected to observe a striped phase at a given a reduced density $\rho r_0^2 = 0.8$.

To test the effective agreement with the molecular dynamic methods, we have first carried out a Monte Carlo simulation suppressing the first term in Eq. (2) and analyzing the classical limit $\Lambda = 0$. The classical simulation is then run picking up an initial random configuration which should be regarded as a fluid state. Subsequently, the thermodynamic equilibrium at a high enough temperature, t_0, is established. We recall that the Monte Carlo steps per particle considered here only comprise Metropolis moves at the analyzed temperature. t_0 has been chosen to have a high acceptance ratio per particle [36]. Then the temperature is decreased gradually $t \to t - \Delta t$ ($\Delta t > 0$), starting with the last configuration sampled at the previous higher temperature. The procedure is completed when the ground state or the wished temperature is approached. By employing this painless annealing strategy, the stripe pattern can be reached for temperatures $t < 0.12$. As an example, Fig. 1(c) shows the final configuration of the procedure reached down to $t = 0.03$ for $N = 512$. We note that the chosen N suffices for reproducing a classical configuration made of stable stripes.

Now we move to discuss the thermodynamic observables and their estimators applied in this study. Regarding the calculation of the kinetic energy in a PIMC contest, it is well know that the evaluation of this estimators can be performed in different ways [27]. In the present paper, we apply the method proposed by Jang *et al.* in Ref. [37]. This choice is appropriated, again keeping in mind the smoothness of the LPG pair potentials. The lack of discontinuities, in fact, does not spoil the approximation adopted for sampling the density matrix of the system.

Structural properties of the stripe phase are analyzed by means of the radial distribution function $g(r)$, which in the PIMC formalism reads

$$g(r) = \frac{1}{2\pi \rho r_0^2 (N-1) r} \left\langle \sum_{i,j \neq i} \delta(r - r_{ij}(\tau)) \right\rangle_\tau , \qquad (4)$$

where and $\langle \ldots \rangle_\tau$ is the average over complex time, τ, trajectories $\mathbf{r}_i(\tau)$ [27]. In a generic modulated pattern or a triangular crystal phase Eq. (4) displays pronounced and wide maximum and, at the same time, well-defined minima. In contrast, a standard superfluid shows a $g(r)$ having the usual liquidlike behavior, that is, a first peak around the averaged interparticle distance followed by a series of damped oscillations around one [38].

A further observable extremely useful in order to address quantum properties of Eq. (2) is the superfluid fraction of the system. Specifically, within the two-fluid model, the superfluidity is obtained taking advantage of the linear response theory by inspecting the different response to boundary motion of the normal component with respect to the superfluid one. Here we implement the estimator proposed a few decades ago by Pollock and Ceperley [39]. Following this, the superfluid fraction as a function of temperature, along the orthogonal directions x and y of the simulated box, yields

$$f_s^{(i)} = \frac{t}{\Lambda^2 \rho r_0^2} \langle w_i^2 \rangle , \qquad (5)$$

where $i = x, y$, and $\langle \ldots \rangle$ stands for the thermal average of the winding number estimator w_i [39]. Differently from an homogeneous superfluid, a density-modulated superfluid (supersolid) presents a nonunitary but uniform response of the estimator in Eq. (5) [17].

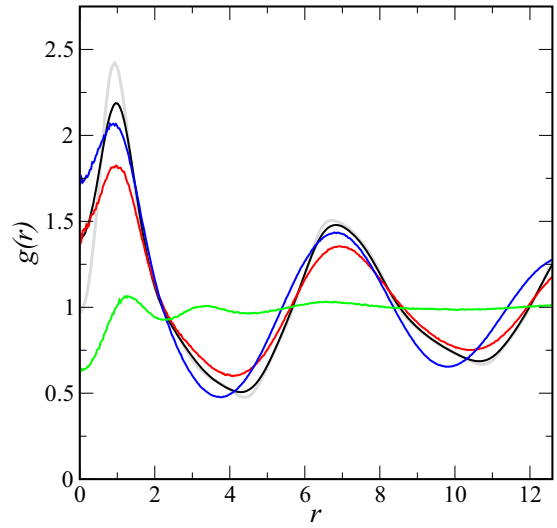

FIG. 2. Radial distribution function $g(r)$ for $\Lambda = 0$ (grey line), $\Lambda = 0.32$ (black line), $\Lambda = 0.45$ (red line), $\Lambda = 0.55$ (blue line), and $\Lambda = 0.77$ (green line).

III. RESULTS

We begin by examining the stability of the stripe patterns increasing Λ. Figure 2 displays the radial distribution function considering some different values of the de Boer parameter. The case for $\Lambda = 0$ (grey line) reproduces the density modulation for the classical system, previously discussed [Fig. 1(c)]. Considering the quantum regime ($\Lambda \neq 0$), one can roughly discern two different behaviors: one referring to modulated phases ($\Lambda = 0.32,\ 0.45,\ 0.55$) and a second ($\Lambda = 0.77$) identifying a superfluid phase. For $\Lambda = 0.32$ and 0.45 (black and red lines, respectively) the stripe phase mainly shows the same modulation of the classical configuration. Yet at $r = 0$, $g(r)$ for $\Lambda = 0.32,\ 0.45,$ and 0.55 turns out to be larger than its classical counterpart. The effect outlines the increasing of the local fluctuations when the Bose–Einstein statistics is taken into consideration. Interestingly, the behavior at $r = 0$ grows stronger about $\Lambda = 0.55$. At the same time, again at $\Lambda = 0.55$, we also obtain a change of density modulation thus marking a cluster solid [the corresponding snapshot configuration is offered in Fig. 3(b)]. In addition, exhibiting a finite superfluid signal, this crystal can be regarded as a supersolid (see below). Finally, for $\Lambda \gtrsim 0.6$, the supersolid evidently gets into a superfluid.

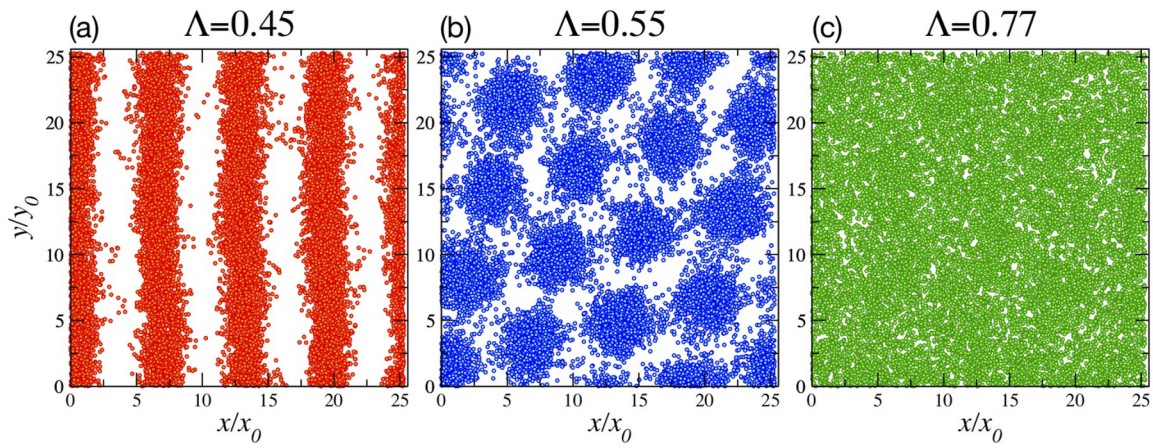

FIG. 3. PIMC's density distribution in real space of three snapshot configurations increasing Λ: (a) stripe phase, (b) supersolid phase, and (c) superfluid phase (see text).

Figure 3 shows snapshots of the projection of world lines onto the xy plane for three different phases, once again modifying the de Boer parameter. Here the system displays a well-defined structural transition about $\Lambda \approx 0.5$, between stripe phase [Fig. 3(a)] and a triangular cluster supersolid [Fig. 3(b)]. Bosons in Fig. 3(a) visibly delocalize themselves along a single stripe and not among nearest-neighbor stripes. This initial analysis looks to exclude the existence of a global coherence, although for properly addressing the issue we have to discuss the estimator of the superfluid fraction (see Fig. 5). As indicated above, Fig. 3(b) shows clear evidence that quantum fluctuations lead to the transition from stripes to supersolid. In Fig. 3(c), we show a configuration made of bosons completely delocalized throughout the box, identify then a superfluid phase ($\Lambda = 0.77$).

A comparison between configurations in Figs. 3(a) and 3(b) can be also qualitatively operated taking into consideration the frequency of cycles of permutations among bosons [40,41]. As one expects, long exchanges of identical particles take place in a system where a nonzero global superfluid response is observed. Not only long exchanges characterize a usual homogeneous superfluid [of which, for instance, Fig. 3(c) is a peculiar example] but also regimes where a spatial broken symmetry may endure, marking then the presence of a supersolid phase [2]. The probability of permutation $P(L)$ involving L bosons (with $1 \leqslant L \leqslant N$) is reported in Fig. 4. $P(L)$ referring to a stripe phase (red histogram) shows that permutations entail cycles to about 130 bosons, that is, approximatively the number of particles located on each stripe. On the contrary, in the supersolid regime (blue histogram), we observe permutations extending themselves over long cycles and almost covering the entire set of particles in the box ($L \lesssim N$).

Figure 5 depicts the superfluid fraction—Eq. (5)—by varying the de Boer parameter. In the stripe phase ($\Lambda \lesssim 0.5$), $f_s^{(i)}$ displays a strong anisotropy. In particular, the superfluid

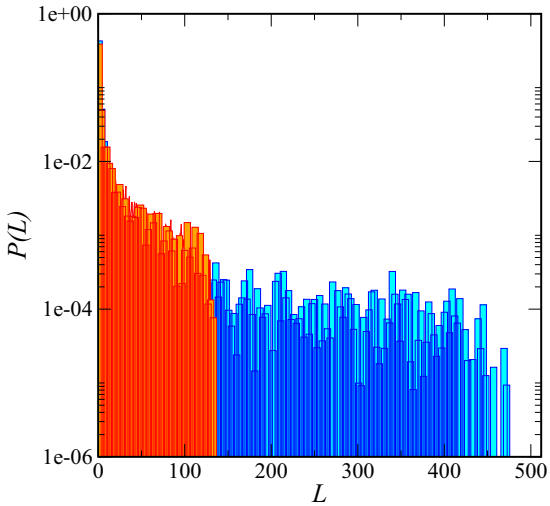

FIG. 4. Frequency of exchange cycles of length L ($1 \leqslant L \leqslant N$) in the stripe phase (red histogram), in which the superfluidity results finite along the stripe direction only, and supersolid phase (blue histogram), in which the superfluidity is uniformly finite throughout the simulated box.

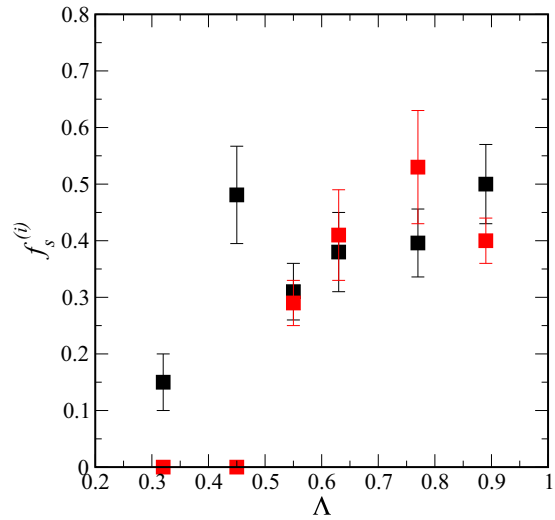

FIG. 5. Superfluid fraction $f_s^{(i)}$, $i = x, y$, as a function of the de Boer parameter along the stripes direction (in this work $f_s^{(y)}$, black square) and orthogonally ($f_s^{(x)}$, red square) to them.

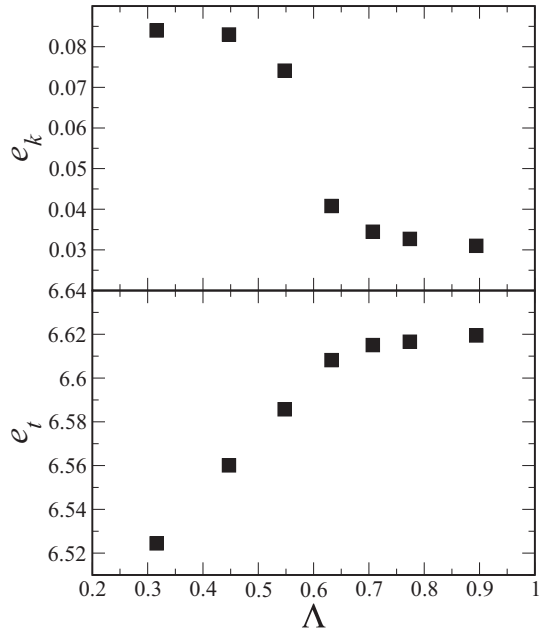

FIG. 6. Kinetic energy (upper panel) and total energy (lower panel) as a function of Λ. Error bars lie within point size.

fraction is finite along the y direction and it vanishes along the x direction ($f_s^{(x)} = 0$ and $f_s^{(y)} \neq 0$, respectively). This result conclusively asserts that each stripe is phase coherent, but globally the system is not or, more precisely, the system behaves like a collection of independent quasisuperfluid chains. It is interesting to mention that the lack of global coherence (i.e., meaning the absences of supersolidity) has also been recently noted on systems of striped dipolar bosons [42].

For $\Lambda \gtrsim 0.5$, the superfluid signal results are finite and uniform along both directions ($f_s^{(x)} \approx f_s^{(y)}$). Considering the fact that we are working at finite temperature, superfluidity cannot help plainly discern between cluster supersolid and superfluid phases. On the other hand, such a demarcation can be easily operated checking up quantities like permutation cycles or equilibrium configurations. Yet, one would tentatively state that f_s at $t = 0.03$ is increasing upon increasing Λ from supersolid to superfluid phase. By all means, superfluidity appears to remain unaffected for $\Lambda \gtrsim 0.65$, that is, when bosons are regarded as completely delocalized throughout the box, signaling then the complete melting of any quantum modulated phase.

Now we examine the stability of the phases discussed so far, introducing some considerations connected to the system's energy. Figure 6 reports the kinetic energy per particle (e_k upper panel) as well as the total energy per particle (e_t lower panel) again versus the de Boer parameter at $t = 0.03$. Total energy shows two different slopes that are related, the first to the ordered phases and the second to the superfluid phase. Regarding the kinetic energy, as one might expect, we observe that e_k decreases when quantum fluctuations get stronger and stronger. The transition between the cluster crystal and a fluid phase is marked by a clear jump about $\Lambda \approx 0.6$, around this value the e_k is halved. At lower Λ, the kinetic energy displays an additional lowering around the transition between stripe and cluster phases; thus also here it sounds reasonable to reaffirm that the effect is mainly driven by quantum fluctuation and quantum mechanical exchanges.

IV. DISCUSSION AND CONCLUSIONS

In this paper, we have investigated the stability of a stripe phase at finite temperature and introducing quantum fluctuations into the system. The stripe pattern formation is classically introduced by considering a two-body LPG potential [13]. For moderate value of the de Boer parameter ($\Lambda \lesssim 0.5$), the stripe phase still survives against the tendency of bosons to delocalize throughout the box. The pattern furnishes a superfluid signal along the stripe direction only, without evidence of any global coherence. The preset results are consistent if compared to a recent study on a two-dimensional system of bosons interacting via a dipole-dipole interaction [42]. In particular, the authors observe crystal stripe phases if dipoles are tilted beyond a certain critical value. Also, for dipolar bosons, the global phase coherence does not emerge and, consequently, without showing any supersolid phase. Interestingly, the analogy between Ref. [42] and the stripe phase introduced by the LPG potential are indeed quite evident. Considering their quantum features, both systems behave as a set of one-dimensional uncorrelated boson Luttinger liquids.

The LPG boson model also shows that quantum fluctuations drive a structural transition from stripe to a cluster triangular crystal, apparently where thermal fluctuation does not play any specific role. Indeed, in the range $0.5 \lesssim \Lambda \lesssim 0.6$, we remark that (i) the competition between quantum fluctuations and the LPG potential tends to remove the degeneration of the Fourier transform of Eq. (1) and to impose a density modulation with a wavelength corresponding to a single equilibrium minima and (ii) quantum-mechanical exchanges of bosons particles act to stabilize the solid phase, as already observed in Ref. [21]. By increasing Λ further, the competition between the two terms get lost and cluster crystals melt into a superfluid.

To conclude, extending the present paper, future work may address how similar complex structures can control quantum-mechanical exchanges, considering other two- or multilengthscale soft-core potentials, possibly applicable in an experimental contest as, for instance, ultracold dipolar atoms [43–50] or supporting the understanding of other engaging systems such as quantum quasicrystals [51–53].

ACKNOWLEDGMENT

The author wishes to thank P. Ziheler and T. Macrì for valuable discussions.

[1] F. Sciortino, Proc. Int. Sch. Phys. "Enrico Fermi" **193**, 1 (2016).

[2] M. Boninsegni and N. V. Prokof'ev, Rev. Mod. Phys. **84**, 759 (2012).

[3] C. N. Likos, A. Lang, M. Watzlawek, and H. Löwen, Phys. Rev. E **63**, 031206 (2001).

[4] H. Shin, G. M. Grason, and C. D. Santangelo, Soft Matter **5**, 3629 (2009).

[5] C. N. Likos, Phys. Rep. **348**, 267 (2001).

[6] C. N. Likos, H. Löwen, M. Watzlawek, B. Abbas, O. Jucknischke, J. Allgaier, and D. Richter, Phys. Rev. Lett. **80**, 4450 (1998).

[7] J.-B. Delfau, H. Ollivier, C. López, B. Blasius, and E. Hernández-García, Phys. Rev. E **94**, 042120 (2016).

[8] M. A. Glaser, G. M. Grason, R. D. Kamien, A. Košmrlj, C. D. Santangelo, and P. Ziherl, Europhys. Lett. **78**, 46004 (2007).

[9] J. Fornleitner and G. Kahl, J. Phys.: Condens. Matter **22**, 104118 (2010).

[10] B. A. Lindquist, R. B. Jadrich, and T. M. Truskett, Soft Matter **12**, 2663 (2016).

[11] M. B. Sweatman and L. Lue, Adv. Theory Simul. **2**, 1900025 (2019).

[12] T. Dotera, T. Oshiro, and P. Ziherl, Nature **506**, 208 (2014).

[13] K. Barkan, M. Engel, and R. Lifshitz, Phys. Rev. Lett. **113**, 098304 (2014).

[14] J. Swift and P. C. Hohenberg, Phys. Rev. A **15**, 319 (1977).

[15] R. Lifshitz and D. M. Petrich, Phys. Rev. Lett. **79**, 1261 (1997).

[16] N. Henkel, R. Nath, and T. Pohl, Phys. Rev. Lett. **104**, 195302 (2010).

[17] F. Cinti, T. Macrì, W. Lechner, G. Pupillo, and T. Pohl, Nat. Commun. **5**, 3235 (2014).

[18] N. Henkel, F. Cinti, P. Jain, G. Pupillo, and T. Pohl, Phys. Rev. Lett. **108**, 265301 (2012).

[19] H. Labuhn, D. Barredo, S. Ravets, S. de Léséleuc, T. Macrì, T. Lahaye, and A. Browaeys, Nature **534**, 667 (2016).

[20] J. Zeiher, R. van Bijnen, P. Schauß, S. Hild, J. yoon Choi, T. Pohl, I. Bloch, and C. Gross, Nat. Phys. **12**, 1095 (2016).

[21] F. Cinti, M. Boninsegni, and T. Pohl, New J. Phys. **16**, 033038 (2014).

[22] M. O. Goerbig, P. Lederer, and C. M. Smith, Phys. Rev. B **69**, 115327 (2004).

[23] G. Pupillo, P. Ziherl, and F. Cinti, Quantum cluster quasicrystals, arXiv:1905.12073.

[24] G. Masella, A. Angelone, F. Mezzacapo, G. Pupillo, and N. V. Prokof'ev, Phys. Rev. Lett. **123**, 045301 (2019).

[25] M. Y. Kagan, *Modern Trends in Superconductivity and Superfluidity* (Springer, Dordrecht, 2013).

[26] M. B. Sevryuk, J. P. Toennies, and D. M. Ceperley, J. Chem. Phys. **133**, 064505 (2010).

[27] D. M. Ceperley, Rev. Mod. Phys. **67**, 279 (1995).

[28] W. Krauth, *Statistical Mechanics: Algorithms and Computations*, Oxford Master Series in Physics (Oxford University Press, New York, 2006).

[29] M. Boninsegni, N. V. Prokof'ev, and B. V. Svistunov, Phys. Rev. E **74**, 036701 (2006).

[30] F. Cinti, P. Jain, M. Boninsegni, A. Micheli, P. Zoller, and G. Pupillo, Phys. Rev. Lett. **105**, 135301 (2010).

[31] F. Cinti, J. Low Temp. Phys. **182**, 153 (2015).

[32] F. Cinti, D.-W. Wang, and M. Boninsegni, Phys. Rev. A **95**, 023622 (2017).

[33] W. Lechner, F. Cinti, and G. Pupillo, Phys. Rev. A **92**, 053625 (2015).

[34] M. Boninsegni, Nikolay Prokof'ev, and B. Svistunov, Phys. Rev. Lett. **96**, 070601 (2006).

[35] S. A. Chin, Phys. Lett. A **226**, 344 (1997).

[36] M. P. Allen and D. J. Tildesley, *Computer Simulation of Liquids* (Oxford University Press, New York, 2017).

[37] S. Jang, S. Jang, and G. A. Voth, J. Chem. Phys. **115**, 7832 (2001).

[38] P. Chaikin, T. Lubensky, and T. Witten, *Principles of Condensed Matter Physics*, Vol. 1 (Cambridge University Press, Cambridge, 2000).

[39] E. L. Pollock and D. M. Ceperley, Phys. Rev. B **36**, 8343 (1987).

[40] A. J. Leggett, *Quantum Liquids Bose Condensation and Cooper Pairing in Condensed-Matter Systems* (Oxford University Press, New York, 2006).

[41] P. Jain, F. Cinti, and M. Boninsegni, Phys. Rev. B **84**, 014534 (2011).

[42] F. Cinti and M. Boninsegni, J. Low Temp. Phys. **196**, 413 (2019).

[43] F. Böttcher, J.-N. Schmidt, M. Wenzel, J. Hertkorn, M. Guo, T. Langen, and T. Pfau, Phys. Rev. X **9**, 011051 (2019).

[44] M. Wenzel, F. Böttcher, T. Langen, I. Ferrier-Barbut, and T. Pfau, Phys. Rev. A **96**, 053630 (2017).

[45] L. Tanzi, E. Lucioni, F. Famà, J. Catani, A. Fioretti, C. Gabbanini, R. N. Bisset, L. Santos, and G. Modugno, Phys. Rev. Lett. **122**, 130405 (2019).

[46] L. Chomaz, D. Petter, P. Ilzhöfer, G. Natale, A. Trautmann, C. Politi, G. Durastante, R. M. W. van Bijnen, A. Patscheider, M. Sohmen, M. J. Mark, and F. Ferlaino, Phys. Rev. X **9**, 021012 (2019).

[47] F. Cinti and M. Boninsegni, Phys. Rev. A **96**, 013627 (2017).

[48] F. Cinti, A. Cappellaro, L. Salasnich, and T. Macrì, Phys. Rev. Lett. **119**, 215302 (2017).

[49] Y. Kora and M. Boninsegni, J. Low Temp. Phys. **197**, 337 (2019).

[50] Y.-C. Zhang, F. Maucher, and T. Pohl, Phys. Rev. Lett. **123**, 015301 (2019).

[51] S. Gopalakrishnan, I. Martin, and E. A. Demler, Phys. Rev. Lett. **111**, 185304 (2013).

[52] J. Hou, H. Hu, K. Sun, and C. Zhang, Phys. Rev. Lett. **120**, 060407 (2018).

[53] K. Viebahn, M. Sbroscia, E. Carter, J.-C. Yu, and U. Schneider, Phys. Rev. Lett. **122**, 110404 (2019).